Publ. Astron. Soc. Japan **35**, 77–86 (1983)

Cyclic Phase Changes of Interstellar Medium

Satoru IKEUCHI

Department of Physics, Hokkaido University, Sapporo 060

and

Hiroyuki TOMITA

College of Liberal Arts, Kyoto University, Sakyo-ku, Kyoto 606

(Received 1982 July 19; accepted 1982 November 5)

Abstract

Based upon the view that the interstellar medium composed of a hot gas, a warm gas, and cold clouds is regulated by supernova remnants, its time variation is studied by use of model equations. Similar to nonlinear oscillators, three types of solutions are found. They are a stable stationary state (focus), a limit cycle, and a runaway state. It is suggested that each solution corresponds to a realistic state of interstellar medium. An entrained state of interstellar medium by an external periodic force shows a chaotic state and/or a new limit-cycle state, depending upon the frequency and the amplitude of the external force. The present result suggests a new approach to the evolution of galaxies.

Key words: Chaotic state; Entrained state; Interstellar medium; Limit cycle.

1. Introduction

By observations of soft X-ray background and O VI absorption lines, it has been indicated that a considerable fraction of interstellar space is occupied by a hot ($\gtrsim 10^{5.5}$ K) rarefied ($\lesssim 10^{-2}$ cm^{-3}) gas. Thus, a picture of the interstellar medium (ISM) has changed from a two-phase model composed of a warm ($\sim 10^4$ K) gas and cold clouds (Field 1965) to a three-phase model including a hot gas (McKee and Ostriker 1977). In a preceding paper (Habe et al. 1981), we investigated the time variation of the interstellar medium, which is regulated by supernova remnants.

In the present paper, we present a set of model equations, which have simplified forms of exact interchange processes among three components of the interstellar medium. By examining the model equations, we can see the property of a stationary state. Similar to nonlinear oscillators and chemically reacting systems, the stationary state bifurcates from a stable focus to an unstable one with a limit-cycle orbit. This behavior is given in sections 2 and 3 including some numerical examples.

In section 4, we study an entrained state by a periodic external force. The entrained state around a stable focus shows a new limit cycle or a forced oscillation with a small amplitude. On the other hand, the entrained state around an unstable focus shows a systematic bifurcation to a chaotic state or a new limit-cycle state, when the frequency of an external force has a special value. This suggests a new instability of an entrained state. These fea-

tures of nonlinear behaviors are discussed in relation to the picture of the ISM and to a new approach to the study of the evolution of galaxies in section 5.

2. Model Equations and Linear Analysis

We assume that the interstellar medium consists of three components, a hot gas, a warm gas, and cold clouds, with fractional masses X_h,X_w, and X_c, respectively. The volume of the galaxy is assumed to be fixed. Their relative abundances are regulated by supernova remnants (SNR) through the following processes: (a) the sweeping of a warm gas into a cold component, (b) the evaporation of cold clouds embedded in a hot gas, and (c) the radiative cooling of a hot gas by collisions with a warm gas. The rate coefficients for these processes have been given by Habe et al. (1981). In the present paper, we simplify these three processes and their rate coefficients in order to meet our purpose to reveal characteristic features of the evolution of the ISM rather than to give quantitative results.

The sweeping rate of a warm gas into a cold component is expressed as (rate of supernova explosions per unit volume)$\times$(average volume of an SNR at the maximum radius)$\times$(abundance of ambient medium). We approximately express it as aX_w, in which a is of the order of $(10^{-13}\ \mathrm{SN\ pc^{-3}\ yr^{-1}})\times 4\pi(50\ \mathrm{pc})^3/3 \simeq 5\times 10^{-8}\ \mathrm{yr^{-1}}$. Although the maximum radius of an SNR depends upon the filling factor of a hot gas component, we fix the coefficient a in the expectation that it does not much affect the results.

The evaporation rate of cold clouds is proportional to the abundance of clouds, the volume fraction, and the temperature of the hot gas component, in which clouds are embedded. By increasing the volume of the hot gas, its temperature also increases, since the supernova explosions may frequently occur inside the SNR cavities. From this consideration, we take the evaporation rate as $bX_cX_h^2$. The coefficient b is a complex function of the supernova rate, the lifetime of an SNR at the evaporation-dominated stage, the average temperature of the hot gas, and the cloud size. It will be of the order of 10^{-7}–$10^{-8}\ \mathrm{yr^{-1}}$.

As the cooling process of the hot gas, we consider that the hot gas in SNR cavities is mixed with the ambient warm gas at the destruction stage of SNRs. Therefore, the cooling rate is assumed to be proportional to the collision rate between the hot and the warm gases as cX_wX_h. The coefficient c will be of the order of 10^{-6}–$10^{-7}\ \mathrm{yr^{-1}}$. Although we should take account of the radiative cooling, which is proportional to X_h^2, we do not include this term from the following consideration. When the hot gas with the temperature $\sim 10^6$ K prevails over the galaxy, it extends many kiloparsecs above the plane, and the associated radiative losses will become ineffective (McKee and Ostriker 1977). We imagine that the state $X_h=1$ corresponds to the galactic wind as mentioned later.

According to the above interchange processes, we obtain a set of rate equations for determining the time variation of each component as

$$\frac{dX_w}{d\tau} = -aX_w + cX_hX_w\,, \tag{1}$$

$$\frac{dX_c}{d\tau} = -bX_cX_h^2 + aX_w\,, \tag{2}$$

$$\frac{dX_h}{d\tau} = -cX_hX_w + bX_cX_h^2\,. \tag{3}$$

Since $X_c+X_h+X_w=1$, we express two independent variables as $X=X_c$ and $Y=X_h$. Further, we normalize the time and the coefficients a and b as $t=c\tau$, $A=a/c$, and $B=b/c$:

$$\frac{dX}{dt}=-BXY^2+A(1-X-Y)\,, \tag{4}$$

$$\frac{dY}{dt}=-Y(1-X-Y)+BXY^2\,. \tag{5}$$

Equations (4) and (5) are similar to those of a chemically reacting system or a biological system. So long as we restrict ourselves to use equations (4) and (5), the method to treat the problem is the same as that developed for the nonlinear behavior of an open system (Glansdorff and Prigogine 1971; Nicolis and Prigogine 1977).

Among three stationary states, i.e.,

$$\text{I:}\quad X_0=(1-A)/(1+AB),\quad Y_0=A\,, \tag{6a}$$

$$\text{II:}\quad X_0=0\,,\quad Y_0=1\,, \tag{6b}$$

$$\text{III:}\quad X_0=1\,,\quad Y_0=0\,, \tag{6c}$$

the first state I is not realized when $A>1$ because of $0\leq X\leq 1$ and $0\leq Y\leq 1$. Examining the flow diagram, each stationary state shows the following properties:

I: A focus for $A<1$ (stable or unstable),
II: A node for $A>1$ and a saddle for $A<1$,
III: A higher order saddle for any A.

In order to see the stability of the focus, the perturbations around the fixed point I are assumed as

$$X=X_0+x\,e^{\omega t}\,,\quad Y=Y_0+y\,e^{\omega t}\,. \tag{7}$$

From the linearized equations for x and y, we obtain the eigenvalue equation for ω as

$$\omega^2+AB(Y_0-X_0)\omega+A^2B(1-A)=0\,. \tag{8}$$

Since the real part of ω is written as

$$\mathrm{Re}(\omega)=\mathrm{Re}\{AB(X_0-Y_0)\pm[A^2B^2(X_0-Y_0)^2-4A^2B(1-A)]^{1/2}\}/2\,, \tag{9}$$

the focus I is stable, i.e., $\mathrm{Re}(\omega)<0$ at $Y_0>X_0$ or

$$B>B_c\equiv(1-2A)/A^2\,. \tag{10}$$

By decreasing B for a fixed A, the focus bifurcates to an unstable focus. As shown in the next section, the limit-cycle orbit is realized at $B<B_c$. Thus, the solutions of equations (4) and (5) are classified into

(i) $A>1$; all the orbits reduce to the node ($X_0=0$, $Y_0=1$),
(ii) $A<1$ and $B>B_c$; they reduce to a stable focus [$X_0=(1-A)/(AB+1)$, $Y_0=A$],
(iii) $A<1$ and $B<B_c$; they reduce to the limit-cycle orbit

These three types of solutions seem to correspond to the following states of the ISM, respectively:

(i) all the gas is transformed to a hot gas ↔ a runaway state,
(ii) a stable stationary state ↔ a stable two-phase (small A and large B) or a three-phase state,
(iii) a nonstationary but stable cyclic orbit ↔ a cyclically changing state.

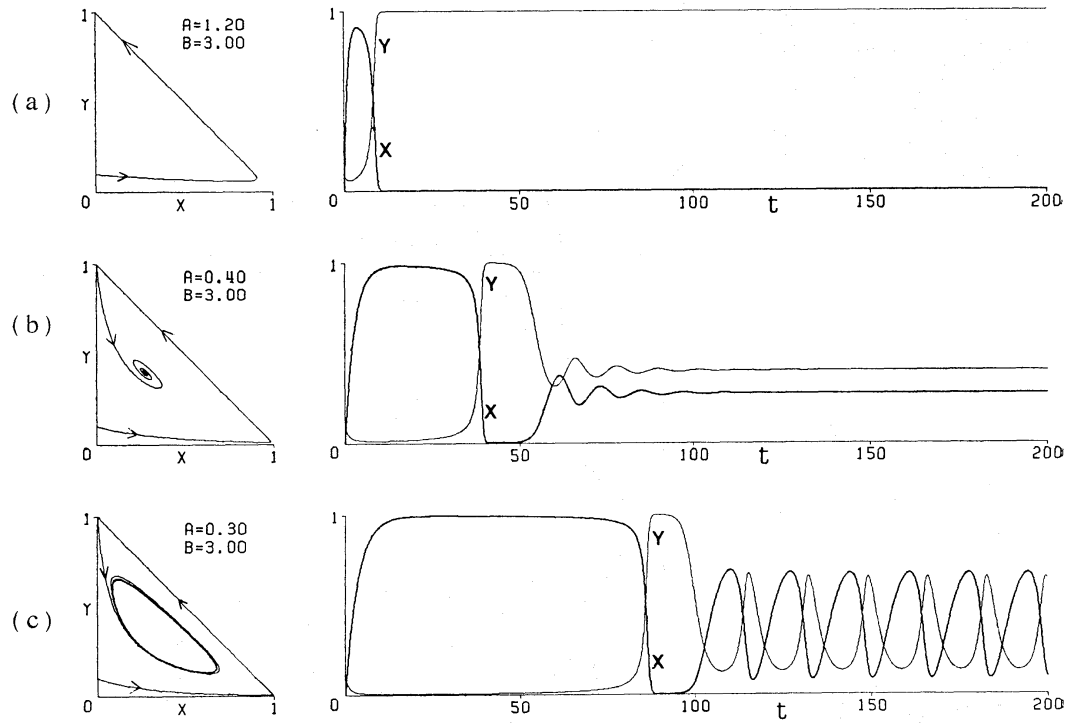

Fig. 1. Typical three orbits in the X–Y plane and time variations of abundances X and Y for (a) node ($A=1.2$, $B=3.0$), (b) stable focus ($A=0.4$, $B=3.0$), and (c) limit cycle ($A=0.3$, $B=3.0$) from the initial point $X_1=0.0$ and $Y_1=0.1$.

These are confirmed by numerical integrations of equations (4) and (5).

3. Numerical Examples

Choosing the initial point arbitrarily as $X_1=0.0$ and $Y_1=0.1$, we calculate the time variations of X and Y. The parameters chosen here are (i) $A=1.2$, $B=3.0$, (ii) $A=0.4$, $B=3.0$, and (iii) $A=0.3$, $B=3.0$, corresponding respectively to the three solutions typical in the preceding section. The phase diagrams are shown in figure 1 for the above three models.

As is seen, in the runaway model all the gas is promptly transformed to a hot gas. It is understood that a large A means efficient sweeping in comparison with the radiative cooling of a hot gas if we remember that A is normalized by the cooling coefficient c. Therefore, the swept gas is first converted into cold clouds and then transformed to a hot gas.

By decreasing A from unity, the channel from a hot gas to a warm gas by radiative cooling operates efficiently, and the network of interchange occurs among three-component functions.

As a result, the stable stationary state is realized at finite X_0 and Y_0. In equations (4) and (5), the term BXY^2 is the highest degree of nonlinearity. If B is rather large, a small change from a stationary value X_0 or Y_0 works as a restoring force within the linear regime and a stable focus is expected as case (b) shown in figure 1. In this case, the orbit in the phase diagram shows a decaying oscillation approaching the focus ($X_0=0.27$, $Y_0=0.40$). We call the frequency of this oscillation the proper frequency, i.e., the imaginary part of the eigenvalue of equation (8).

Decreasing A requires a large deviation from the stationary value so as to complete the network. As a result, the nonlinearity turns a stable focus into an unstable one. In the

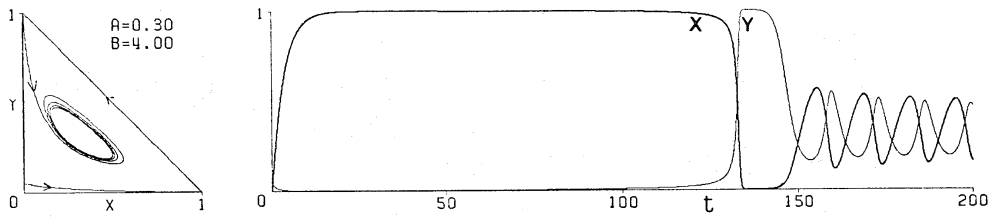

Fig. 2. The same as in figure 1 but for $A=0.3$ and $B=4.0$ from $X_i=0.0$ and $Y_i=0.05$. The initial prolonged metastable states are remarkable.

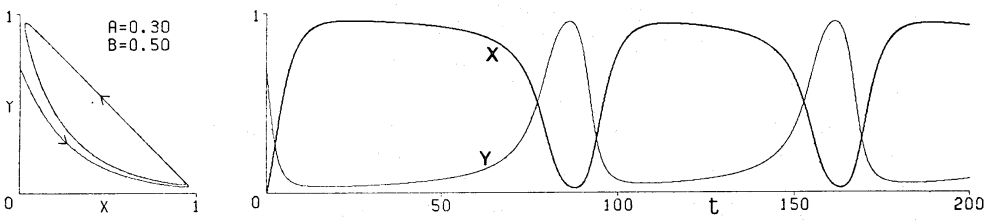

Fig. 3. The same as in figure 1 but for $A=0.3$ and $B=0.5$ from $X_i=0.0$ and $Y_i=0.7$. The orbit in X–Y plane slowly approaches the limit cycle with a large amplitude and a small frequency.

present model, Poincare–Bendixon's criterion for the existence of a limit cycle is satisfied at the unstable focus. Therefore, for any initial values the oribit always reduces to a limit cycle, whose amplitude and frequency are determined by A and B.

In order to see the dependence of the properties of a limit cycle upon the coefficient B, we show the results for $B=4.0$ and 0.5 in the case of $A=0.3$. As is seen in figures 2 and 3, two remarkable features are indicated. One is that the amplitude and the period of a limit cycle increase with decreasing B from the critical value B_c, as readily understood. The other is that the cloud component keeps a high mass fraction longer than the hot gas. This comes from the fact that the exchange rate becomes very small near the point $X\simeq 1$ and $Y\simeq 0$. Apparently, a metastable state with a pure cloud phase or a pure hot gas phase appears in turn. This property seems to reproduce the intermittent activity indicated in dwarf galaxies, where the interchange rates A and B are considered to be as small as those adopted in figure 3.

Furthermore, it should be noted that in the present initial condition we observe a prolonged, metastable state ($X\simeq 1.0$, $Y\simeq 0.0$) in the first place, and then an active phase ($X\simeq 0.0$, $Y\simeq 1.0$) follows before attaining the stable limit cycle with a small amplitude as in figures 1c and 2. In these models, the assumed initial condition corresponds to an almost warm-gas phase, which may be attainable in an early galaxy. This gas is once transformed to cold clouds, a part of which collapses to stars. After that, frequent supernova explosions make the interstellar medium into a hot phase. Therefore, the evolutionary feature as in figure 2 may display the active era of young galaxies. In order to see this in detail, we should examine the time variation of coefficients A and B. This is beyond the model equations of this paper.

4. Entrained State

In galaxies, some additional interchange processes are expected such as the forced conversion from a warm gas to clouds due to the shock wave associated with a spiral arm, the ionization of clouds due to the stellar UV flux, and the gas escape due to the tidal interaction

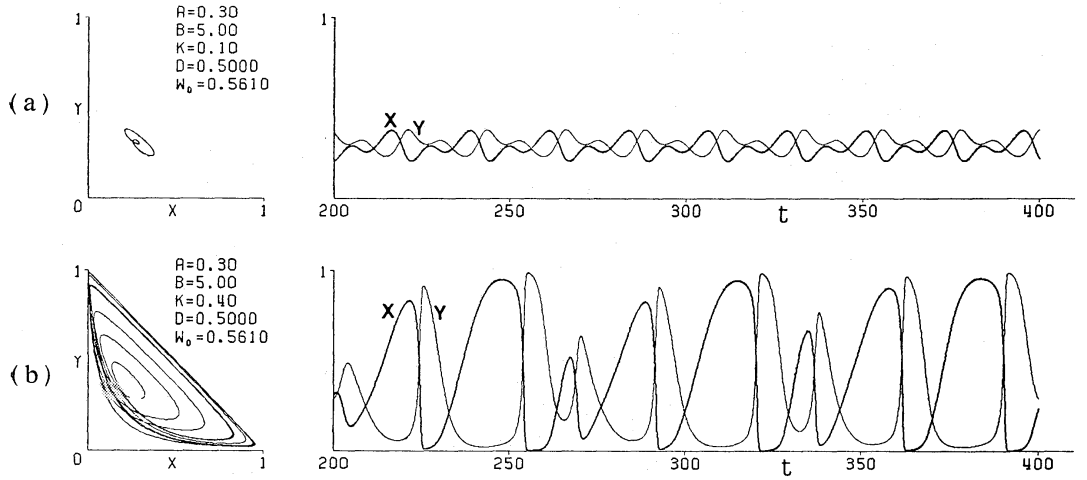

Fig. 4. A double limit cycle (a) and chaotic orbit (b) of an entrained state from the stable focus $X_1=0.28$ and $Y_1=0.30$ for $A=0.3$ and $B=5.0$. The amplitude and frequency of an external force are $K=0.1$ (a) and $K=0.4$ (b), and $D=\Omega/\Omega_p=0.5$.

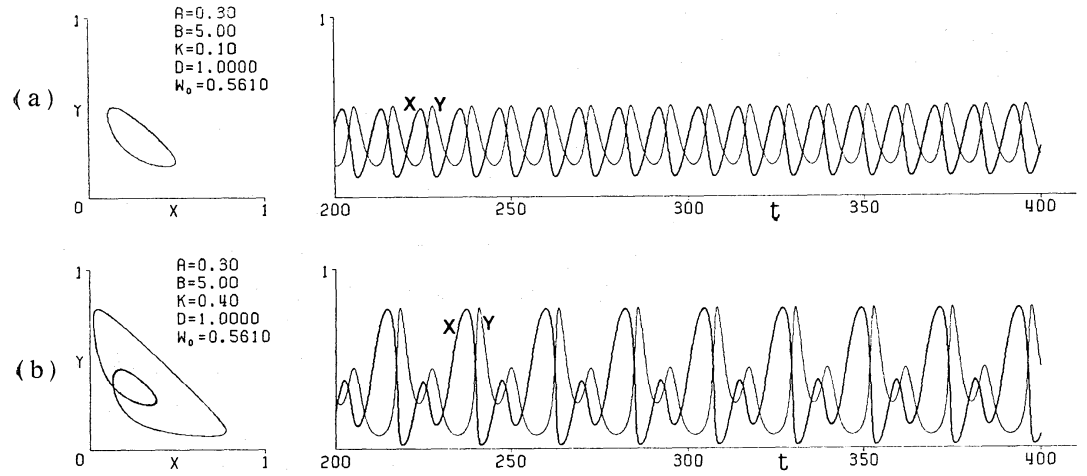

Fig. 5. The same as in figure 4 but for (a) $K=0.1$ and $D=1.0$ and (b) $K=0.4$ and $D=1.0$. A single limit cycle clearly bifurcates to a double limit cycle with increasing K.

with a nearby galaxy. Here we study effects of a periodic external force on the rate of interchange between a warm gas and clouds, analogous to the entrainment in chemically reacting systems. Here, we suppose the warm gas is enforced to convert to clouds with a frequency Ω as a model of the galactic shock wave. Then, equation (4) changes to

$$\frac{dX}{dt}=A(1-X-Y)[1+K\cos(\Omega t)]-BXY^2\,, \tag{11}$$

where K is the amplitude of the external force. In this expression, we assume the conversion rate of the warm gas is proportional to its abundance. This is different from the entrainment studied by Daido and Tomita (1979).

In the first place, we study the entrainment of a stable focus. As an example, we take the parameters $A=0.3$ and $B=5.0$ and set the focus ($X_0=0.28$, $Y_0=0.30$) as the initial model. The frequency of an external term is measured in units of the proper frequency $\Omega_p(=0.5610)$.

Within the ranges of parameters K and $D \equiv \Omega/\Omega_p$ investigated in the present calculation, we find the following characteristics of entrainment:

(1) When $D=\Omega/\Omega_p=1/2$, a double limit cycle with two different amplitudes are observed at $K \leq 0.2$ and they appear in turn with the frequency Ω_p as in figure 4. With increasing K ($K>0.4$), a regular limit cycle is interrupted for a time interval, in which the ratio $X(t)/Y(t)$ shows two oscillations of small amplitudes, and the orbits seem to be quasi-periodic.

(2) In the resonant case $\Omega=\Omega_p$, a single limit cycle with a rather large amplitude is found at $K \leq 0.2$. With increasing K, a single limit cycle seems to bifurcate to a double ($K=0.4$) limit cycle as in figure 5b.

(3) In the case of $D=\Omega/\Omega_p>1$, the entrained state is wholly goverened by the external term. A limit cycle with a very small amplitude and with the frequency Ω is realized for any K.

(4) At ranges $D<0.5$ and $0.5<D<1.0$, the entrained state asymptotically approaches a single limit cycle with the frequency $\Omega=D\Omega_p$.

The above results mean that even if the stable equilibrium is attained in the interstellar medium it is enforced to change the cyclic state due to a periodic external force. Especially, when the ratio of the external frequency to the proper one, D, is $n/2$ (n: integer), the amplitude of the resultant limit cycle is very large, i.e., $|X-X_0|$ and $|Y-Y_0| \gg K$, and its frequency coincides with the external one $\Omega=n\Omega_p/2$.

Second, we study the entrainment of a limit cycle by an external force. As an example, we adopt the case of $A=0.3$ and $B=3.0$ and set the point on the limit cycle $X_1=0.27$ and $Y_1=0.60$ as the initial model. The characteristics of an entrained state, which we find in the present calculations, are as follows:

(1) In the case of a small amplitude ($K=0.1$), the special entrainment is found as a multiple limit cycle with the frequency $\Omega_p(=0.37355)$ for $D=\Omega/\Omega_p=1/n$ ($n=1,2,3,\ldots$), and its multiplicity is n. The examples are shown in figure 6.

(2) Furthermore, a regular, multiple limit cycle is realized for $D=\Omega/\Omega_p=n/m$ (n,m; integer) and its multiplicity is usually m. Therefore, when $m=1$, a single limit cycle is found for any n. Although the frequency of the limit cycle modulates a bit, it is not entrained to the external frequency.

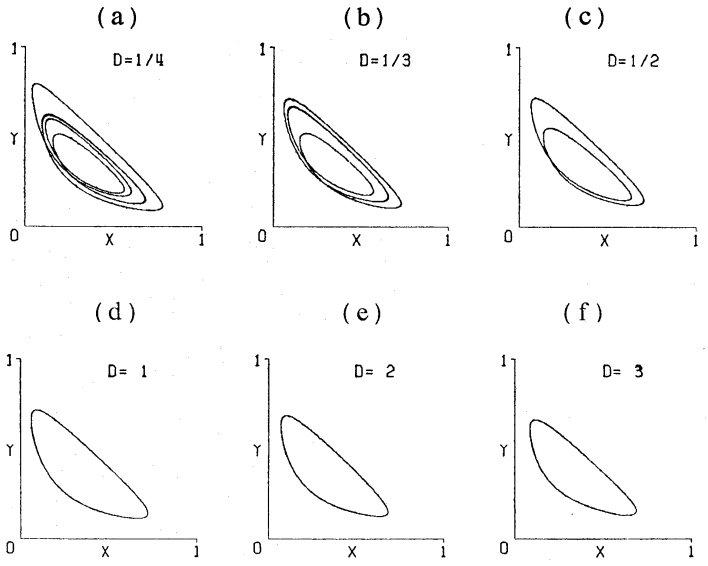

Fig. 6. Examples of a multiple limit cycle for $A=0.3$ and $B=3.0$. The external amplitude is fixed as $K=0.1$, but its frequency varies as (a) $D=1/4$, (b) 1/3, (c) 1/2, (d) 1, (e) 2, and (f) 3. Each multiplicity is exactly m for $D=n/m$ (n, m: integers).

(3) Except for the above frequencies, the orbits in the phase plane are random, but limited to restricted space. At present, we cannot clarify whether the orbits are simply aperiodic or chaotic. As an example, we show the results for the case of a small perturbation $K=0.1$ and $D=1/\sqrt{2}$. The orbit seems to be chaotic, but it is concluded to be quasi-periodic, because a strobo map of succeeding values of X and Y at time intervals $2\pi/\Omega$ shows apparently a closed loop as in figure 7b. Therefore, the attractor of the orbits is a kind of

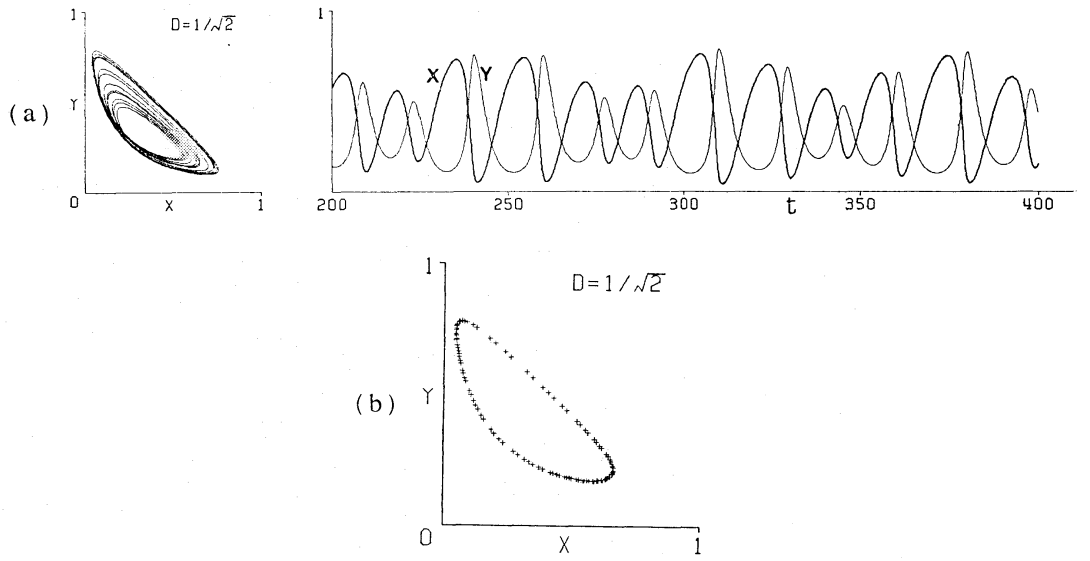

Fig. 7. (a) Quasi-periodic orbit for the case of $K=0.1$ and $D=1/\sqrt{2}$. (b) Strobo map of succeeding values of X and Y at a time interval $2\pi/\Omega$.

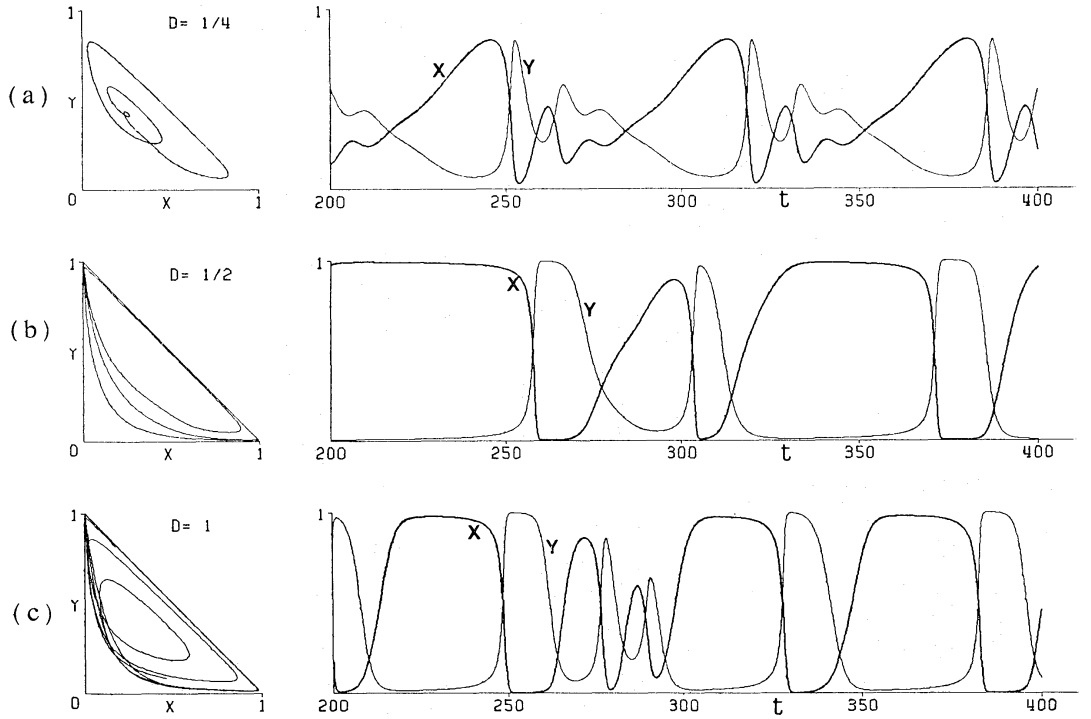

Fig. 8. The chaotic orbits for the case of a large amplitude, $K=0.5$. The external frequencies are taken as (a) $D=1/4$, (b) 1/2, and (c) 1.

torus, not a strange attractor.

(4) With increasing K, the regular pattern of the entrained state begins to be destroyed from the lower-frequency side. For example, the single limit cycle is stable at $\Omega=2\Omega_p$ even if $K\gtrsim 0.5$, but the entrained state at $\Omega/\Omega_p\leq 4/3$ is almost chaotic at $K=0.5$. As shown in figure 8, a multiple limit cycle is recognized for $\Omega=\Omega_p/4$, but the orbits are irregular for $\Omega=\Omega_p/2$ and Ω_p. In the latter cases, the orbits approach intermittently to saddle regions ($X\simeq 1.0$, $Y\simeq 0.0$) and ($X\simeq 0.0$, $Y\simeq 1.0$), where time variations of X and Y become slow. This can be regarded as one of orbital instabilities, i.e., two close points in the initial state are separated with time, especially, after every passage through the saddle regions.

(5) Astrophysically the above entrainment is interesting in relation to a prolonged metastable state of the interstellar medium. The external force enforces the interstellar medium to get into the slowly changing state $X\simeq 1$ and $Y\simeq 0$, in which the burst of star formation is expected. This case will be applied to the tidal interaction between galaxies. Due to the induced shock wave, the warm gas is wholly transformed to clouds. After two galaxies passed through, the external term disappears and the burst of star formation is expected.

Since we examine the model equations for the interchange processes, the numerical values of K and $D=\Omega/\Omega_p$ have no physical meaning by themselves. However, the physical nature of the present results are applicable to the evolution of interstellar medium. One is that an entrained state with the single limit cycle ($\Omega/\Omega_p=n$) due to an external force shows a large-amplitude change even if the external force is weak ($K\simeq 0.1$). Second, a double limit cycle suggests that the interstellar medium can take two phases of an active phase and a quiet phase in turn. These two will be reinterpreted in relation to the gradients of activity of star formation rates in our Galaxy. Third, it is seen that an encounter into a nearby galaxy can bring the galaxy to an active phase.

The above implications will be verified by a simulation in a realistic model of a galaxy. At the same time, a more detailed study of an entrained state with respect to the amplitude, the frequency, and the initial phase of an external term will be given elsewhere.

5. Conclusions

By using a simple set of model equations for the interchange processes of the interstellar medium, we found several new characteristics of its evolution. Especially, the cyclic phase change expressed as a limit cycle in the present model is plausible, because galaxies with the same gas mass but with different activities are frequently indicated. This is simply understood by considering that we observe galaxies at different phases (Fujimoto and Ikeuchi 1983).

At the same time, we predict the runaway state of the interstellar medium at a high A, in which the hot gas prevails all over the galaxy. This may be the reason why the neutral gas is not observed in elliptical galaxies. For the model of a small A and B, the frequency of the limit cycle, which corresponds to the speed of evolution, is small but its amplitude is large. This means that the galaxy with a low supernova rate shows a slow evolution but a distinct change of the star formation rate. This feature well corresponds to dwarf galaxies. Therefore, the observed characteristics of various galaxies may be explained by the interchange rates. It is to be noted that the values of A and B do not directly correspond to the supernova rate but depend upon the absolute value of ambient gas density. They show effective rates of the interchange processes.

In the case of spiral galaxies, two possibilities for the formation of spiral arms have been proposed. One is that the spiral arms are formed by the self-gravity of the galaxy such

as the density wave theory. In this case, the evolution of the interstellar medium is entrained by the periodic, gravitational potential of the arm. The features shown in section 4 may qualitatively be applicable. The other possibility is that the spiral arms are the self-organized, diffusive structures originated in the interchange processes and the diffusive effects of the interstellar medium. This idea is similar to that by Seiden and Gerola (1979), but the present model is deterministic but not stochastic. In a succeeding paper, we will discuss the formation of a structure in nonequilibrium galaxies.

We thank Professor S. Sakashita for his continuous encouragement.

References

Daido H., and Tomita. K. 1979, *Prog. Theor. Phys.*, **61**, 825.
Field, G. B. 1965, *Astrophys. J.*, **142**, 531.
Fujimoto, M., and Ikeuchi, S. 1983, submitted to *Publ. Astron. Soc. Japan.*
Glansdorff, P., and Prigogine, I. 1971, *Thermodynamic Theory of Structure, Stability and Fluctuations* (Wiley-Interscience, London), pp. 210–215.
Habe, A., Ikeuchi, S., and Tanaka, Y. D. 1981, *Publ. Astron. Soc. Japan*, **33**, 23.
McKee, C. F., and Ostriker, J. P. 1977, *Astrophys. J.*, **218**, 148.
Nicolis, G., and Prigogine, I. 1977, *Self-Organization in Nonequilibrium Systems* (John Wiley and Sons, Inc., New York), chap. 6.
Seiden P. E., and Gerola, H. 1979, *Astrophys. J.*, **233**, 56.